

DATA FUSION OF SINGLE-TAG RFID MEASUREMENTS FOR RESPIRATORY RATE MONITORING

W. Mongan*, R. Ross*, I. Rasheed†, Y. Liu†, K. Ved†,
E. Anday‡, K. Dandekar†, G. Dion§, T. Kurzweg†, and A. Fontecchio†

*College of Computing and Informatics: Drexel University, Philadelphia, PA USA

†College of Engineering: Drexel University, Philadelphia, PA USA

‡Department of Pediatrics: Drexel University College of Medicine, Philadelphia, PA USA

§Westphal College of Media Arts and Design: Drexel University, Philadelphia, PA USA
{wmm24, rr625, ir54, yl636, kuv23, ea32, krd26, gd63, tk48, af63}@drexel.edu

Abstract—Using wireless, passive, wearable, knitted, smart garment devices, we monitor biofeedback that can be observed via strain gauge sensors. This biofeedback includes respiratory activity, uterine monitoring during labor and delivery, and regular movements to prevent Deep Vein Thrombosis (DVT). Due to noise artifacts present in a wireless strain gauge monitor and the possibly non-stationary nature of the signal itself, signal analysis beyond the Fourier transform is needed to extract the properties of the observed motion artifacts. We improve the utility of a single Radio Frequency Identification (RFID) tag by fusing multiple features of the tag, in order to precisely determine the frequency and magnitude of motion artifacts. In this paper, we motivate the need for a multi-feature approach to RFID-based strain gauge analysis, correct raw RFID interrogator measurements into features, fuse those features using a Gaussian Mixture Model and expectation maximization, and improve respiratory rate detection from 9 to 6 mean squared error over prior work.

I. INTRODUCTION

RFID was originally designed for identity recognition only, limiting the need for computing and memory resources on an RFID chip [1]. Inventory-based RFID tracking technology typically polls for RFID tags within a certain radius of the interrogator, and those tags confirm their presence by responding with their electronic product code (EPC). More recently, researchers have explored other uses for RFID, which require additional information from the chip. For example, researchers have used RFID to track the position and velocity of a product in order to perceive when customers move a product in a store [1], and used a fixed array of RFID tags to detect and track untagged objects which move through the array [2].

We combine a knitted antenna with a single 900 MHz Murata MAGICSTRAP RFID tag and embed the pair into a wearable smart garment device. We then poll the tag 50-100 times a second [3], [4] and monitor for changes in the Received Signal Strength Indicator (RSSI), Doppler shift, and phase of the tag. We have used this system to monitor uterine contractions, analyze respiration, and monitor DVT motion [5]. In this paper, we report on using the system to measure respiration rate.

There are four primary ways to measure respiration rate:

- **flow**: measuring the physical movement of air in and out of the respiratory tree through an airtight mask placed over the subject's mouth and nose,

- **ETCO₂**: measuring the change in the partial pressure of CO₂ in air near the entrance to the respiratory tree with a sensor placed near the subject's mouth and nose,
 - **acoustic**: measuring vibrations in the neck which are associated with respiration by placing sensors on the subject's neck, and
 - **change in abdominal size**: measurement of changes to the circumference of the abdomen resulting from the expansion and contraction of the lungs and/or diaphragm by placing sensors on the subject's abdomen and/or chest.
- Currently most hospital monitoring devices are wired and cumbersome. In contrast, our system is wireless and relatively unobtrusive, tracking changes in abdominal size (see Figure 1).



Fig. 1. We use a knit-fabric antenna (made with conductive thread) and an RFID tag as a strain gauge sensor.

In previous efforts, we have detected sleep apnea on a programmable baby mannequin after 10 seconds of inactivity [6], in accordance with the definition of sleep apnea [7]. To detect apnea, we utilized a t-test on the mean of the power spectral density (PSD) of the Fast Fourier Transform (FFT) of short windows of the time-series data. The mean magnitude of the PSD tends toward zero in the absence of periodic activity in the signal; a t-test determines if this magnitude is significantly below that of the training period (*i.e.*, 30 seconds). We assume that normal respiratory activity takes place during the training period. If the sliding window utilized by the FFT is sufficiently short (*i.e.*, 0.5 seconds), then the windows can be used to estimate the respiratory rate by observing the frequency with which the classified respiratory state changes over time. Respiratory rate was measured for multiple programmed breathing rates with an overall root mean square error of 9 breaths per minute, using a single-feature detection approach [6]. Noise artifacts and respiratory rate transitions contributed to the error, but it is also possible that

an abnormally short or long breath was incorrectly detected, particularly if oscillatory activity bled into more than one window.

Unrelated movements by the subject are captured in-band by changes to the RSSI. This contributes noise that may be eliminated by adding a reference tag on the body that would not be subject to stretching during respiratory motion, something we expect to do in the future. In this effort, we improve on our previous results by fusing together multiple analyses from a single tag, in order to best optimize the estimated rate obtained using minimal infrastructure. A single tag and antenna assembly is used to minimize surface area of the body reserved for sensing. Previously, we created a software infrastructure [8] to collect single-tag data features from the RFID tag. With this infrastructure, we now add one or more measurement approaches of respiratory rate, and fuse those “measures” together to obtain a more precise estimate of the respiration rate. Fusion of the measures is done using Expectation Maximization (EM) within and between the fusion measures, by considering each measurement in time as a point estimate with a variance equal to the recent variance of that measure. The most likely respiratory rate is chosen from the mixture of the Gaussian distributions formed about those point estimates. This method allows a fused estimate to be obtained from even a single measure, by considering its recent estimates as Gaussian point estimates for data fusion.

In this paper, we perform harmonic and non-harmonic feature extraction from an RFID-based strain gauge biosensor, correct each measure at the physical layer, and fuse these measures for real-time respiratory rate estimation using a single physical RFID tag. The rest of this paper is organized as follows: we review related work in Section II, detail our technical approach in Section III, summarize our experimental results in Section IV, and conclude in Section V.

II. RELATED WORK

A. RFID History

Passive RFID was first used during World War II to distinguish between friendly aircraft returning to base and enemy aircraft on the attack. Research continued after the war, but the first commercial use of RFID did not take place until the late 1980s, when various governments began to use RFID for traffic management. By the early 2000s, RFID tags were being used to collect tolls automatically in 3500 traffic lanes in the US. RFID technology has been used to track materials through the supply chain, grant employees card access to secure buildings, and keep track of patients and supplies in hospitals [9], [10]. In the 2000s, researchers began using additional data from RFID tags (read rate, RSSI, phase, and Doppler) and applying machine learning (ML) techniques to accomplish tasks such as robot localization [11] and perception of an object’s state change [12]. These researchers use familiar ML techniques and tools: feature identification and Support Vector Machines.

B. Wireless Respiration Detection History

Recently, researchers have discerned respiration rate wirelessly by measuring changes in abdominal size. Respiration rate has been measured successfully using signals in the 5.5-7.25 and 2.4 GHz range [13], [14]. For example, the WiBreathe system in [15] uses wireless signals to estimate respiration rate without the need for instrumentation on the human body. This system has the advantage of using the same frequency as commercial WiFi devices. However, it lacks a way to uniquely identify readings from multiple patients since there are no identifying features in the reflected WiFi signals.

C. Using RFID for Wireless Respiration Detection

We chose to use a signal in the RFID Ultra High Frequency (UHF) bandwidth (902-928 MHz) for two reasons. First, RFID’s greater wavelength (≈ 33 cm) is more robust against non-respiratory movements (*i.e.*, the subject shifting positions), while still allowing observation of respiratory movement smaller than 1 cm. Second, each tag has a unique identifier (TID) assigned during the manufacturing process [16], which allows for encoded subject identification. Our approach utilizes a single receiving antenna that is subject to frequency hopping in the United States per FCC regulations, as opposed to previous methods which use multiple receiving antenna [13], [14] and may not require frequency hopping.

III. APPROACH

RSSI is a nonstandard measure and subject to perturbations due to frequency hopping. Therefore, the backscatter power $P_{Rx,reader}$ is modeled by Equation 1 [17] in a manner that incorporates the interrogation wavelength λ .

$$P_{Rx,reader} = P_{Tx,reader} \times G_{reader}^2 \times G_{tag}^2 \left(\frac{\lambda}{4\pi r} \right)^4 \times R \quad (1)$$

$P_{Rx,reader}$ is the reported RSSI, which we convert from dBm to Watts via $P_{Rx,reader} = 10^{\left(\frac{RSSI}{10}\right)} \times 1000$. $P_{Tx,reader}$ is a constant defined as 1 Watt (30 dBm) by the interrogator configuration. $G_{reader} = 9$ dBic to reflect a constant reader gain. R is the backscattered-transmission loss, and r is the distance from the interrogator to the tag.

The only factors of the backscatter model affected by strain gauge motion about the RFID tag and knitted antenna are G_{tag} , r , and R . Thus, Equation 2 defines those terms of the backscatter model that are affected by strain gauge motion in terms of the RSSI $P_{Rx,reader}$ and interrogation wavelength λ :

$$\zeta = \frac{r^4}{G_{tag}^2 \times R} = \frac{P_{Tx,reader} \times G_{reader}^2}{P_{Rx,reader}} \times \left(\frac{\lambda}{4\pi} \right)^4 \quad (2)$$

ζ is converted back from Watts to dBm to maintain consistency with the units reported by the interrogator by computing $10 \log_{10}\left(\frac{\zeta}{1000}\right)$. Thus, ζ tracks those terms that are affected by changes in antenna shape or interrogation radius (G_{tag} , r , and R), given the RSSI and interrogation frequency.

Other efforts have re-purposed RFID for coarse motion tracking applications [1]. These efforts used the variations in

the tag velocity for strain sensor monitoring via stretching of the tag. Because RFID signal strength decays quickly (within 5-10 meters), localization with signal strength alone is insufficient. Thus, phase-based location monitoring is also employed for RFID-based localization [18]. Doppler-based velocity calculation is more susceptible to noise than phase-based velocity [1]. However, phase-based computations require a fixed interrogation frequency because phase difference calculations require both interrogations to have the same frequency. Due to Federal Communications Commission regulations [19], we iterate every 200 *ms* over each of 50 frequencies in the 902-928 MHz band. Thus, Doppler-based velocity computations are used so that the interrogation frequency can be accounted for as shown in Equation 3.

The use of observed Doppler shift as a tag velocity measure is less accurate than the phase-based approach. However, we receive better resolution from the Doppler-based velocity measure given that the frequency changes at a rate of 5 Hz, with a read rate of 40-100 Hz that may be split across multiple tags. To mitigate the noise effects inherent in the Doppler signal, the data is smoothed using a Savitzky-Golay filter [20]. We assume that the tag is not perpendicular to the reader. As seen in Equation 3, if the tag is perpendicular to the reader, the cosine term goes to zero. The Doppler frequency is in the form of 16-bit two's complement with four fractional bits and units of Hertz. The Doppler frequency shift value is converted to Hertz by subtracting 65536 from it if the two's complement is greater than 32767 and dividing it by 16. A slower reader configuration was used for interrogation [8], because longer measurement intervals (*i.e.*, longer packet durations) enable increased Doppler shift resolution and more accurate velocity estimation [21].

For a non-perpendicular interrogation angle $\alpha \neq \frac{\pi}{2}$, the radial velocity of the RFID tag v is derived from the Doppler shift f_m of the tag, the interrogation frequency f , and speed of light c , as shown in Equation 3 [21]:

$$v = \frac{c \times f_m}{2f \times \cos\alpha} \quad (3)$$

A. Feature Measures for Respiratory Activity Classification

Using the channel-calibrated RSSI ($\zeta = \frac{r^4}{G_{tag}^2 \times R}$) and velocity measures for Doppler and phase, respectively, we identify features that are suited for different types of respiratory behavior, and fuse them to estimate respiratory rate. These features include spectral analysis using Quinn FFT interpolation and a Hidden Markov Model to track slow deviations from the respiratory frequency. They also include a correlation measure between the first order difference of the RSSI and of the phase observations to identify the beginning and end of each breath. Spectral analysis may indicate oscillatory activity during periods of non-breathing because of the oscillatory nature of the signal. Therefore, hypothesis testing on the Short-Time Fourier Transform (STFT) magnitude is used to detect non-breathing as in previous efforts to detect sleep apnea [6], overriding spectral rate detection results.

1) *Correlating the Velocity and ζ* : Perturbations in the tag velocity are observed from “ambient” motion artifacts, such as moving the torso while breathing or walking about. To separate ambient motion artifacts from the oscillatory respiratory signal under consideration, the velocity measure is fused with the RSSI of the signal. A rolling root mean squared (RMS) of the resulting velocity-time series vector was computed. The rolling RMS gives a measure of the intensity of the motion by measuring the magnitude shift in the signal. Peak detection is employed on the first-order difference of the resulting smoothed velocity RMS vector. Inflection points consisting of the largest slopes upward or downward are identified in the RMS difference signal, as shown in Figure 2, and a strain motion such as an inhalation or expiration is inferred during these periods. A square wave is produced identifying periods of time between the inflection points to denote these periods of motion. Peak detection is a useful alternative to spectral analysis, to correct for situations in which spectral leakage results in a loss of precision.

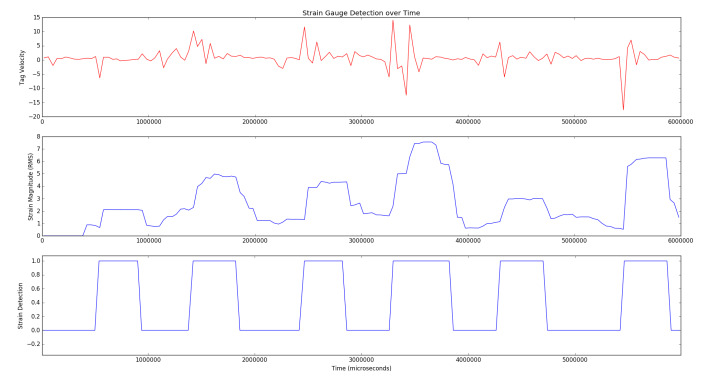


Fig. 2. Square wave showing the periods in between the local maximum and minimum peaks on the first-order-difference of the velocity (top), by detecting large slopes in the rolling root-mean-square (middle) of the velocity signal and converted to a square wave (bottom)

2) *Spectral Analysis*: To overcome the spectral leakage potentially present in the small window, Quinn FFT interpolation is utilized to identify a “frequency offset” between the identified frequency bin and the surrounding frequency bins [22]. A t-test based on a short training period of respiratory activity determines whether the power spectral density indicates respiratory activity, so that these frequency-based approaches are omitted when no motion activity is present [6].

For breathing classification (*i.e.*, apnea detection), we use a short time window (*i.e.*, 0.5 seconds) for the power magnitude, and compare that magnitude to the mean found during a training period. The challenge here is that if the rate changes, there will be more low-magnitude power STFT windows skewing the confidence. So, we check that a greater number of these STFT magnitudes is too low before declaring apnea.

The RFID stream returned from respiratory or subject motion activity represents a non-stationary stochastic process, because the mean and variance of the time-series data depends upon the rate of motion observed at that time. However, the

process is nearly stationary over a short time window, because that window will either include no motion activity (white noise only), or will contain one or few motion artifacts at some spacing interval. In these situations, a STFT can be used to capture the fundamental frequency and amplitude of the motion. However, the short window yields lower resolution in the frequency domain, yielding a quantized frequency as the magnitudes bleed into the surrounding frequency bins. Additionally, the STFT may not recover the fundamental frequency precisely if the stationary assumption is not met, and can conflate noise for signal if the target motion is not present in the window.

Using a frequency-normalized RSSI measure, we perform an STFT to extract the fundamental frequency. A short window is selected in order to mitigate distortion due to non-stationarity of the signal. Thus, frequency resolution is sacrificed for the STFT. We address this reduction in resolution by interpolating across FFT frequency and magnitude bins. Specifically, we utilize local mean spectral density and Quinn’s frequency interpolation [22]. The resulting interpolated peak frequency is provided as an input to a Hidden Markov Model (HMM) that tracks the frequency progression over time to determine the most likely sequence of underlying frequencies exhibited by the subject [23], [24]. To identify the fundamental frequency, we perform Quinn interpolation on each of the frequencies corresponding to peak FFT magnitudes, and then perform a Baum-Welch Forward-Backward posterior probability calculation to find the most likely frequency given the preceding frequency progression [23], [25]. A band-pass filter is applied to ensure that only biologically-feasible frequencies specific to the application are considered (*i.e.*, 0-2 Hz for respiratory activity). If no feasible frequency is obtained through the HMM, either because no peak FFT frequency is found in the current time step, or because there is no likely progression of frequency states that results in the current frequency observation, the chain is re-initialized to assume that all frequencies are equally probable. As a result, this algorithm does not attempt to resolve the case in which no oscillatory activity is present. Instead, a t-test on the magnitude of the STFT power spectrum is used to detect the cessation of respiratory activity by monitoring the spectral density of the signal as a whole over time [6]. The combined algorithm utilizing Quinn interpolation [22] and HMM tracking [23] to obtain the fundamental frequency from spectral analysis of the normalized RSSI is used to augment traditional FFT peak frequency detection, and is shown in Figure 3. We compare Quinn interpolation against a locally weighted average of neighboring locally maximal STFT magnitudes using a local mean spectral density.

B. Multi-Feature Data Fusion

To fuse the individual measures of spectral density, tag velocity, and non-harmonic peak detection, into a coherent estimate of respiratory rate, we model the recent history of each feature measurement as a Gaussian distribution component, and fuse those components via a Gaussian Mixture Model

(GMM). Each measure is then weighted by its likelihood within the GMM, and the resulting respiratory estimate is a weighted average of the individual measures. That estimate is tracked using a Kalman filter to produce the final rate estimate.

Sensor fusion is implemented with a layered approach, even though only a single RFID tag is used to track movement. First, individual measures are corrected against one another. For example, spectral analysis is augmented with historical knowledge of the change in frequency via a Hidden Markov Model, as described in Section III-A2, and noise artifacts present in the RSSI measure are corrected using the time-correlated phase observation, as described in Section III-A1. Then, each measure is fused via its recent history by fitting its recent observations as a Gaussian distribution. Measurement noise may not be Gaussian; however, the variance observed across all measures should be constant if they exhibit the same accuracy. Agreement across sensors is facilitated by fitting these Gaussian distributions to a GMM, even if the observations themselves are not Gaussian, via each measure’s likelihood score within the GMM. Thus, a single measure can be improved by fusing observations temporally with itself.

IV. RESULTS

We programmed a Laerdal SimBaby mannequin to breathe at a pre-defined rate (*i.e.*, 31, 15, 0, 15, and 31 bpm for one minute each). Software sensors observed features from the RFID interrogator such as the RSSI, Doppler, and phase, and corrected them as described in Section III. An Analysis of Variance (ANOVA) test was applied to the uncorrected and corrected estimates.

First, accuracy of single-event respiratory detection was considered. The SimBaby mannequin takes approximately 0.5 seconds to complete a single inspiration or expiration (average of 0.56 seconds observed). Using 0.56 as a ground truth, we detected the beginning and end of each inspiration and expiration, using 1) corrected RSSI ζ , 2) tag velocity estimated from Doppler shift, and 3) the correlation between the two. We observed a Root Mean Squared from ground truth of 1.22 seconds using ζ alone, 0.56 seconds using the velocity measure alone, and 0.57 seconds using the correlation. Thus, the velocity improved significantly over the ζ measure alone (ANOVA test $p = 0.0001$), and short term detection of respiratory behavior is provided primarily by the velocity measure.

When monitoring respiratory rate in the long term, we observed false positives using the velocity measure alone. Using the SimBaby mannequin, we counted the number of respiratory movements (inspiration and expiration) using the velocity alone, ζ alone, and the correlated measure in each six second time window. We observed an RMS of 4.2 respirations for using velocity, 1.7 respirations using ζ , and 1.9 respirations using the correlation, a significant improvement over the velocity measure (ANOVA test $p = 0.001$). By correlating ζ with the velocity measure, we are able to detect both the start of respiratory activity and the respiratory rate.

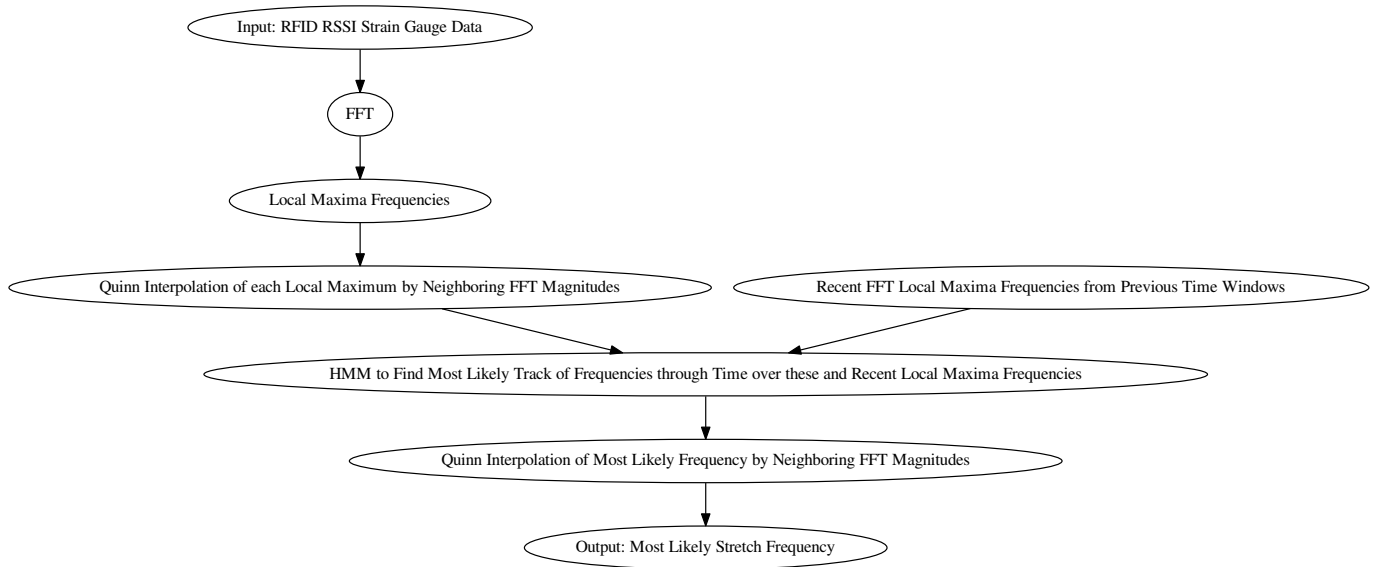


Fig. 3. An algorithm to compute the most likely oscillatory frequency from a time-series window of frequency-normalized RFID RSSI strain gauge data; here, changes in RSSI oscillations are tracked in the frequency domain using a Hidden Markov Model to identify the most likely subject respiratory rate given recent perturbations in RSSI as well as recent historical RSSI oscillatory frequencies

For tracking of long-term respiratory rate, we performed human subject experimentation under an approved IRB protocol, in which the subject breathed normally at an approximate rate of 30 per minute for 30 seconds, followed by 15 per minute for 30 seconds. An FFT with and without Quinn interpolation was used, and was compared against the FFT with Hidden Markov Model frequency bin tracking. Using the subject’s estimated breathing rate as ground truth, we found a Root Mean Squared error of 11 for the FFT alone, 78 with Quinn interpolation, 6 with HMM tracking, and 7 with Quinn interpolation and HMM tracking. HMM tracking without Quinn interpolation outperformed FFT spectral analysis alone, and HMM tracking was able to correct for errors observed during Quinn interpolation.

Fusing these spectral and frequency counting methods, we observe that individual measures are generally corrected via a Kalman-filtered expectation maximization estimate from a Gaussian Mixture Model, even when using only that single measure. For example, the Mean Squared Error for the FFT with Quinn interpolation and HMM tracking measure is reduced from 7 to 6 respirations, with a reduction in variance from 53 to 39. The Mean Squared Error for the FFT with HMM tracking measure is reduced below 6, with a reduction in variance from 30 to 24. The Kalman filter and Gaussian distribution for each measure considers the recent tracking of the measured value, which accounts for the observed improvement. The overall fused Mean Squared Error using a peak counting approach, STFT weighted frequency by mean spectral density, and FFT with Quinn interpolation and HMM tracking, was below 6 (see Figure 4). The local mean spectral density weighted average more precisely estimated the ground truth respiratory rate.

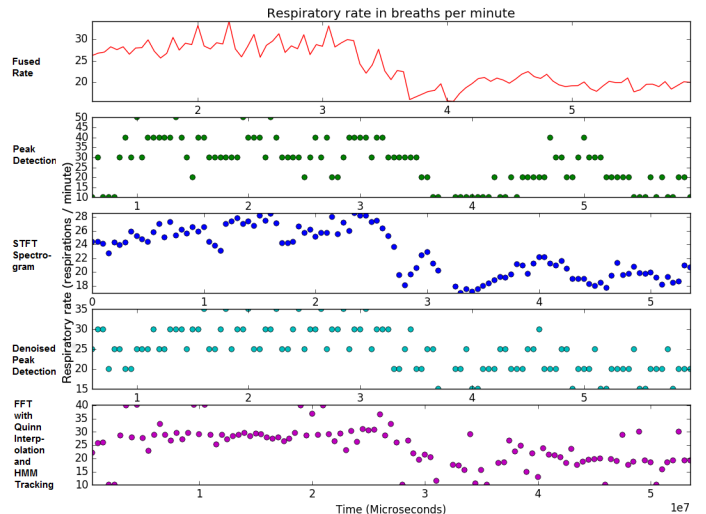


Fig. 4. Individual observed measures and their fusion over time for a human subject breathing at a rate of approximately 30 for 30 seconds, and at a rate of approximately 15 for 30 seconds

V. CONCLUSION AND FUTURE WORK

In this paper, we utilized a single, physical, RFID-based, knitted antenna strain gauge sensor to estimate respiratory rate. We made this estimation by observing the physical properties of RFID interrogations over time, including RSSI, phase, and Doppler shift. We corrected these physical observations for mandatory “channel hopping” by calculating ζ from the measured RSSI, and the velocity v from the observed Doppler shift or phase. These observations were then correlated with one another to correct for noise perturbations in the individual sensor observations as well as against each observation’s

temporal history via a Hidden Markov Model. Finally, individual rate estimates were fused against their own temporal histories as well as against one another via a Gaussian Mixture Model, resulting in an overall respiratory rate estimation. Rate accuracy was measured experimentally, using corrected sensor observations and their uncorrected counterparts, fusion approaches for single measures over time and across multiple measurements.

In the future, we plan to build on these feature measurements in order to detect instantaneous changes in respiratory behavior; for example, predicting the start time of the next breath. Additionally, we are exploring the use of multiple interrogator-antenna-tag systems on a single subject, one located so that it distorts with respiration (*i.e.*, on the abdomen) and one “reference tag” located so that it does not (*i.e.*, on the shoulder) for de-noising.

ACKNOWLEDGMENT

Our research results are based upon work supported by the National Science Foundation Partnerships for Innovation: Building Innovation Capacity (PFI:BIC) subprogram under Grant No. 1430212. Any opinions, findings, and conclusions or recommendations expressed in this material are those of the author(s) and do not necessarily reflect the views of the National Science Foundation. Research reported in this publication was supported by National Institute of Biomedical Imaging and Bioengineering of the National Institutes of Health under award number U01EB023035. The content is solely the responsibility of the authors and does not necessarily represent the official views of the National Institutes of Health. The authors acknowledge support from the Commonwealth of Pennsylvania through the Commonwealth Universal Research Enhancement (CURE) program.

REFERENCES

- [1] J. Han, H. Ding, C. Qian, D. Ma, W. Xi, Z. Wang, Z. Jiang, and L. Shangguan, “CBID: A Customer Behavior Identification System Using Passive Tags,” in *2014 IEEE 22nd International Conference on Network Protocols*, Oct 2014, pp. 47–58.
- [2] H. Ding, M. Xi, Z. Li, and J. Zhao, “Device-free Mobile Target Tracking Using Passive Tags,” *International Journal of Distributed Sensor Networks*, vol. 2015, pp. 12:12–12:12, Jan. 2016. [Online]. Available: <https://doi.org/10.1155/2015/870204>
- [3] D. Patron, W. Mongan, T. P. Kurzweg, A. Fontecchio, G. Dion, E. K. Anday, and K. R. Dandekar, “On the Use of Knitted Antennas and Inductively Coupled RFID Tags for Wearable Applications,” *IEEE transactions on biomedical circuits and systems*, vol. 10, no. 6, pp. 1047–1057, 2016.
- [4] Y. Liu, A. Levitt, C. Kara, C. Sahin, G. Dion, and K. R. Dandekar, “An improved design of wearable strain sensor based on knitted RFID technology,” in *2016 IEEE Conference on Antenna Measurements Applications (CAMA)*, Oct 2016, pp. 1–4.
- [5] W. Mongan, E. Anday, G. Dion, A. Fontecchio, K. Joyce, T. Kurzweg, Y. Liu, O. Montgomery, I. Rasheed, C. Sahin *et al.*, “A Multi-Disciplinary Framework for Continuous Biomedical Monitoring Using Low-Power Passive RFID-based Wireless Wearable Sensors,” in *Smart Computing (SMARTCOMP), 2016 IEEE International Conference on*. IEEE, 2016, pp. 1–6.
- [6] W. M. Mongan, I. Rasheed, K. Ved, A. Levitt, E. Anday, K. Dandekar, G. Dion, T. Kurzweg, and A. Fontecchio, “Real-time Detection of Apnea via Signal Processing of Time-series Properties of RFID-based Smart Garments,” in *Signal Processing in Medicine and Biology Symposium (SPMB), 2016 IEEE*. IEEE, 2016, pp. 1–6.
- [7] R. Begg and M. Palaniswami, *Computational intelligence for movement sciences: neural networks and other emerging techniques*. IGI Global, 2006.
- [8] W. M. Mongan, I. Rasheed, K. Ved, S. Vora, K. Dandekar, G. Dion, T. Kurzweg, and A. Fontecchio, “On the Use of Radio Frequency Identification for Continuous Biomedical Monitoring,” in *International Conference on Internet-of-Things Design and Implementation (IoTDI)*, vol. 2, no. 1. ACM, 2017, pp. 197–202.
- [9] K. Domsouzis, B. Kumar, and C. Anumba, “Radio-Frequency Identification (RFID) Applications: A Brief Introduction,” *Adv. Eng. Inform.*, vol. 21, no. 4, pp. 350–355, Oct. 2007. [Online]. Available: <http://dx.doi.org/10.1016/j.aei.2006.09.001>
- [10] C. Roberts, “Radio Frequency Identification (RFID),” *Computers & Security*, vol. 25, no. 1, pp. 18 – 26, 2006. [Online]. Available: <http://www.sciencedirect.com/science/article/pii/S016740480500204X>
- [11] K. Yamano, K. Tanaka, M. Hirayama, E. Kondo, Y. Kimuro, and M. Matsumoto, “Self-localization of mobile robots with rfid system by using support vector machine,” in *Intelligent Robots and Systems, 2004.(IROS 2004), Proceedings. 2004 IEEE/RSJ International Conference on*, vol. 4. IEEE, 2004, pp. 3756–3761.
- [12] H. Li, C. Ye, and A. P. Sample, “Idsense: A human object interaction detection system based on passive uhf rfid,” in *Proceedings of the 33rd Annual ACM Conference on Human Factors in Computing Systems*. ACM, 2015, pp. 2555–2564.
- [13] F. Adib, H. Mao, Z. Kabelac, D. Katabi, and R. C. Miller, “Smart Homes That Monitor Breathing and Heart Rate,” in *Proceedings of the 33rd Annual ACM Conference on Human Factors in Computing Systems*, ser. CHI ’15. New York, NY, USA: ACM, 2015, pp. 837–846. [Online]. Available: <http://doi.acm.org/10.1145/2702123.2702200>
- [14] C. Chen, Y. Han, Y. Chen, H. Q. Lai, F. Zhang, B. Wang, and K. J. R. Liu, “TR-BREATH: Time-Reversal Breathing Rate Estimation and Detection,” *IEEE Transactions on Biomedical Engineering*, vol. PP, no. 99, pp. 1–1, 2017.
- [15] R. Ravichandran, E. Saba, K. Y. Chen, M. Goel, S. Gupta, and S. N. Patel, “Wibreathe: Estimating respiration rate using wireless signals in natural settings in the home,” in *2015 IEEE International Conference on Pervasive Computing and Communications (PerCom)*, March 2015, pp. 131–139.
- [16] Impinj, “How Does RFID Work?” <https://www.impinj.com/about-rfid/how-does-rfid-work/>.
- [17] Z. Su, S. C. Cheung, and K. T. Chu, “Investigation of Radio Link Budget for UHF RFID Systems,” *Proceedings of 2010 IEEE International Conference on RFID-Technology and Applications, RFID-TA 2010*, no. June, pp. 164–169, 2010.
- [18] P. V. Nikitin, R. Martinez, S. Ramamurthy, H. Leland, G. Spiess, and K. V. S. Rao, “Phase based spatial identification of UHF RFID tags,” in *2010 IEEE International Conference on RFID (IEEE RFID 2010)*, April 2010, pp. 102–109.
- [19] U.S. Government Publishing Office, “Electronic Code of Federal Regulations, Title 47, Chapter I, Subchapter A, Part 15.247,” http://www.ecfr.gov/cgi-bin/text-idx?node=pt47.1.15&rgn=div5#se47.1.15_1247.
- [20] A. Savitzky and M. J. E. Golay, “Smoothing and Differentiation of Data by Simplified Least Squares Procedures.” *Anal. Chem.*, vol. 36, no. 8, pp. 1627–1639, Jul. 1964. [Online]. Available: <http://dx.doi.org/10.1021/ac60214a047>
- [21] Impinj, “Application Note - Low Level User Data Support,” https://support.impinj.com/hc/en-us/article_attachments/200774268/SR_AN_IPJ_Speedway_Rev_Low_Level_Data_Support_20130911.pdf.
- [22] B. Quinn, “Estimation of frequency, amplitude, and phase from the DFT of a time series,” *IEEE Transactions on Signal Processing*, vol. 45, no. 3, pp. 814–817, 1997. [Online]. Available: <http://ieeexplore.ieee.org/lpdocs/epic03/wrapper.htm?arnumber=558515>
- [23] T. Gunes and N. Erdol, “HMM Based Spectral Frequency Line Tracking: Improvements and New Results,” in *2006 IEEE International Conference on Acoustics Speech and Signal Processing, ICASSP 2006, Toulouse, France, May 14-19, 2006*. IEEE, 2006, pp. 673–676. [Online]. Available: <https://doi.org/10.1109/ICASSP.2006.1660432>
- [24] R. L. Streit and R. F. Barrett, “Frequency line tracking using hidden Markov models,” *IEEE Trans. Acoustics, Speech, and Signal Processing*, vol. 38, no. 4, pp. 586–598, 1990. [Online]. Available: <https://doi.org/10.1109/29.52700>
- [25] L. R. Welch, “Hidden Markov Models and the Baum-Welch Algorithm,” *IEEE Information Theory Society Newsletter*, vol. 53, no. 4, Dec. 2003.